Comparative Theoretical Study of H2 Eley–Rideal Recombination Dynamics on W(100) and W(110)

ARTICLE *in* THE JOURNAL OF PHYSICAL CHEMISTRY C · JUNE 2014

Impact Factor: 4.77 · DOI: 10.1021/jp501679n

4 AUTHORS:

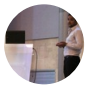

Rémi Pétuya
Donostia International Physics Center
9 PUBLICATIONS **12** CITATIONS
SEE PROFILE

C. Crespos
Université Bordeaux 1
29 PUBLICATIONS **419** CITATIONS
SEE PROFILE

Ernesto Luis Quintas-Sánchez
Observatoire de Paris
7 PUBLICATIONS **27** CITATIONS
SEE PROFILE

Pascal Larregaray
CNRS / Université Bordeaux
67 PUBLICATIONS **612** CITATIONS
SEE PROFILE

THE JOURNAL OF PHYSICAL CHEMISTRY C

Article

pubs.acs.org/JPCC

Comparative Theoretical Study of H_2 Eley–Rideal Recombination Dynamics on W(100) and W(110)

R. Pétuya,[†,‡] C. Crespos,*[,†,‡] E. Quintas-Sanchez,[†,‡,§] and P. Larrégaray[†,‡]

[†]Université de Bordeaux, ISM, CNRS UMR 5255, 33405 Talence Cedex, France

[‡]CNRS, ISM, UMR5255, F-33400 Talence, France

[§]InSTEC, Ave. Salvador Allende esq. Luaces, 10600 La Habana Cuba

ABSTRACT: Quasiclassical molecular dynamics simulations are performed to study the Eley–Rideal recombination of H_2 on two crystallographic planes of tungsten. Potential energy surfaces, based on density functional theory, are used to describe the H+H/W(100, 110) interactions. The calculations are carried out within the single adsorbate limit under normal incidence of the impinging H atoms. The influence of the crystallographic anisotropy on reaction cross sections and energy distribution of the formed molecules is analyzed in detail. Despite some discrepancies in the dynamics of recombination between W(100) and W(110) surfaces, translational, rotational, and vibrational energies of the formed molecules do not depend significantly on surface symmetry. Vibrational distribution of formed H_2 molecules are found in good agreement with experiments.

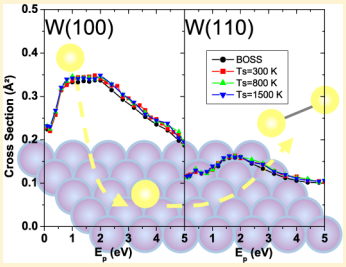

1. INTRODUCTION

The understanding of elementary processes at the gas–solid interface is of great interest in many domains, as for example in chemistry of atmospheric[1,2] and interstellar media,[3,4] heterogeneous catalysis,[5−7] plasma–wall interactions.[8,9] The last 20 years have revealed an important fundamental interest in the dynamics of molecular recombination on metal surfaces. Numerous experimental[10−12] and theoretical[13−30] works have analyzed the mechanisms involved in hydrogen recombination on metals. This reaction, usually non activated and largely exothermic, provides highly excited molecules[10−12] of potential interest for the production of negative ions sources for thermonuclear fusion.[31,32] Many of the molecular recombinations proceed via the so-called hot atom (HA) and/or Eley–Rideal (ER) mechanisms. For both mechanisms, an impinging atom from the gas phase (projectile) collides with an adsorbed one (target) to produce the molecule, the distinction between HA and ER being the diffusion time of the projectile above the surface prior to reaction with the target. In the HA process, the projectile is initially trapped onto the surface and experiences several rebounds before colliding with the target. In contrast, the ER mechanism involves a rather direct encounter between both atoms.[19,20,23,25,33−36] In the present work, a theoretical study of the ER hydrogen recombination on the W surface is proposed within the zero coverage limit where the direct encounter mechanism is expected to play a major role. Indeed, because of the projectile diffusion step, the HA reaction cross section is expected to decrease with the lowering of preadsorbed species coverage. Although theoretically suggested in the 1940s,[37−39] the ER process has only been experimentally demonstrated 50 years later by the ultrahigh vacuum (UHV) molecular beam experiments of Rettner and Auerbach for the case of H(D) reacting with a D(H) atom preadsorbed on Cu(111).[10,12] The experimental study of molecular hydrogen recombination on tungsten walls started in the late 1980s,[40,41] using various detection techniques (REMPI, dissociative electron attachment process) to characterize the highly excited formed molecules. In these experiments, H_2, vibrationally excited up to $v = 5$[41] and $v = 9$[40] quantum states, were observed. Recently, experiments[42] were performed on a polycrystalline tungsten surface. Like in early works, highly excited H_2 has been observed and attributed to ER recombination with H atoms adsorbed in low energy binding sites. A theoretical investigation of H_2 ER recombination on W(100) using quasiclassical trajectories (QCT) simulations[30] has also been developed. However, the accuracy of the tight-binding potential energy surface (PES) used can be challenged, as the most stable adsorption site was erroneously found to be the 4-fold hollow site whereas it is settled, both experimentally[43] and theoretically,[44,45] that the H atoms preferentially bind on the bridge position for this system.

In this paper, the analysis of ER recombination of H_2 molecules on tungsten is theoretically revisited via QCT calculations on accurate full-dimensional density functional theory (DFT) based PESs for both W(100) and W(110) crystallographic planes. In particular, the effect of surface symmetry on the reactivity is scrutinized. Indeed, understanding the crystallographic anisotropy is a key issue of surface science. It has been shown that W(100) and W(110) planes exhibit different behaviors regarding the dissociative adsorption dynamics of H_2.[45] Though several studies have investigated the effect of the crystallographic plane on H_2 recombination on metals,[33,46−51] no such studies exist for the recombination on W. As a consequence, the objective of the present work is 2-

Received: February 17, 2014
Revised: April 16, 2014

   dx.doi.org/10.1021/jp501679n | J. Phys. Chem. C XXXX, XXX, XXX–XXX

fold: (i) performing a comparative analysis of the ER recombination cross section for both surfaces, and (ii) checking if notable differences on H_2 ro-vibrational excitation are observed when going from W(100) to W(110).

The paper is structured as follows. Methodology and details of the calculations are presented in section 2. In section 3, the results of the ER dynamics are discussed for both crystallographic planes. A comparison with recent experimental measurements is proposed in section 4. Finally, we conclude in section 5.

2. METHODOLOGY

The normal incidence scattering of atomic hydrogen over H-preadsorbed W surfaces is investigated within the zero coverage limit (single adsorbate), using a QCT approach. The details of the methodology which are conveyed in previous papers[52,53] are only briefly summarized here. Within the Born−Oppenheimer approximation, dynamics are simulated on a single electronic ground-state PES. Because of ultrafast ER reaction times (subpicosecond time scale), electron−hole pair excitations are neglected.[54] H atoms are depicted in the Cartesian reference frame displayed in Figure 1 with the origin

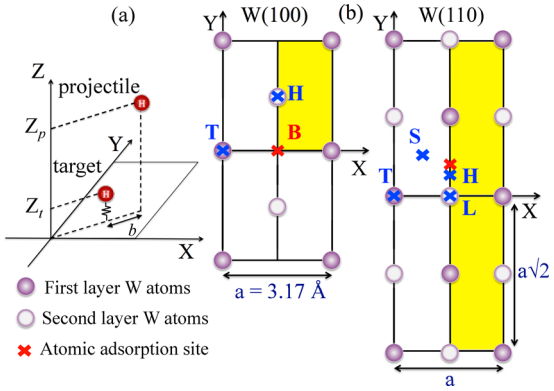

Figure 1. (a) Coordinates of the H+H/W system. The Cartesian frame origin is located on a tungsten top surface atom. Z_p and Z_t are respectively the altitude of the projectile and the target, and b is the impact parameter. (b) W(100) and W(110) surfaces with some specific surface sites (a is the lattice constant parameter of 3.17 Å): T, top; B, bridge; H, hollow; L, long bridge; S, short bridge. The most stable atomic adsorption sites are represented in red. The yellow areas are the sampling areas of the (X,Y) initial positions of the projectiles.

on a tungsten top surface atom. The Z axis is defined normal to the surface and the (X,Y) axes lie on the surface plane unit cell. For H+H/W(100) and H+H/W(110), flexible periodic London−Eyring−Polanyi−Sato (FPLEPS) potentials[55−57] have been used to model the interaction of the H atoms with an infinite and periodic surface. For the H+H/W(110) system, the accuracy of the FPLEPS model was recently tested in comparison with a PES constructed with an adaptation of the corrugation reducing procedure (CRP)[58−60] to study the ER abstraction dynamics.

As in previous works,[52,53] simulations have been first performed within the Born−Oppenheimer Static Surface (BOSS) approximation. Furthermore, a general Langevin oscillator (GLO)[61−65] was used to model the surface temperature effects and the energy exchanges with the W surface. Within this model, the motion of surface atoms is described via a three-dimensional harmonic oscillator coupled to a thermal bath to account for energy dissipation into the bulk. The W(100) surface is known to undergo structural phase transition, below 200 K,[66,67] leading to a c(2 × 2) zigzag atomic rearrangement, whereas at higher temperatures, the unreconstructed (1 × 1) structure is observed. This unreconstructed (1 × 1) surface (Figure 1) is considered in this work; therefore, temperature effects are only examined above 200 K.

The most stable position of the adsorbed H atom on W(100) is on the bridge site (B: $X = a/2$, $Y = 0$, with a lattice parameter a = 3.17 Å) at 1.20 Å above the surface with a binding energy of 3.08 eV (3.09 eV in ref 45 and 3.08 eV in ref 68). On W(110), the most stable site for atomic adsorption is located very close to the 3-fold hollow site on $X = a/2$ and Y = 0.634 Å, at 1.096 Å above the surface with binding energy of 3.07 eV (3.06 eV in ref 45).

The initial conditions of QCT simulations are identical to the ones used in a previous work. The target initially sits in the most favorable adsorption site with an energy equal to the zero-point energy (ZPE) calculated through a X, Y, and Z mode decomposition. The initial vibrational phase of the target is sampled randomly. Values used for the ZPE along X, Y, and Z modes, in reasonable agreement with experiments,[43,69−71] are displayed in Table 1. The projectile atom starts at Z_p = 7.0 Å, in

Table 1. Values of the ZPE along X, Y, and Z Axes (given in meV) for H/W(100) and H/W(110) Systems

system	Z	X	Y
H/W(100)	67	55	33
H/W(110)	68	55	55

the asymptotic region of the potential, with normal incidence. Influence of the initial perpendicular collision energy of the projectile, E_p, is studied within the range 0.1−5.0 eV. Taking advantage of the symmetry of each system, the (X,Y) initial coordinates of the projectiles are randomly sampled in the yellow areas indicated in Figure 1. For the H+H/W(100) system, 320 000 trajectories are performed to reach convergence of the ER cross section, whereas for the H+H/W(110) system, 640 000 trajectories are used for each collision energy. The ER cross section reads:

$$\sigma_r = A \int\int_D P_r(X_p, Y_p) dX_p dY_p$$

with integration over D, the sampling yellow area in Figure 1 and A = 4 (A = 2) for H+H/W(100) (H+H/W(110)). $P_r(X_p,Y_p)$, the two-dimensional opacity function, is the density of probability of ER recombination for a given set of X_p and Y_p which denote the initial position of the projectile.

Exit channels of the simulations are defined in detail elsewhere.[52,53] A recombination event is classified as ER whenever the formed molecule reaches the initial altitude of the projectile with positive center-of-mass momentum along Z. As the calculations are performed within the single adsorbate limit, HA recombination cannot be simulated here.

3. DYNAMICS RESULTS AND DISCUSSION

Cross sections for ER abstraction are presented in Figure 2 as a function of the initial perpendicular energy of the projectile, E_p, for different temperatures and within the BOSS approximation. As in previous works on hydrogen recombination on other metals,[18,26,28] cross sections are small, with maxima about 0.33 Å^2 (0.14 Å^2) for H+H/W(100) (H+H/W(110)). ER reactivity

dx.doi.org/10.1021/jp501679n | J. Phys. Chem. C XXXX, XXX, XXX−XXX

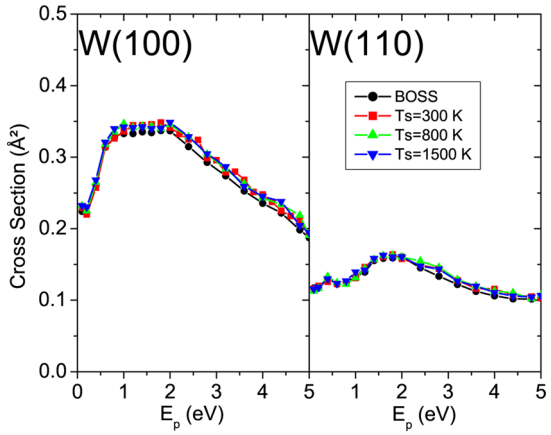

Figure 2. Cross sections in (Å^2) for ER abstraction within the BOSS model and the moving surface model at T_s = 300, 800, and 1500 K as a function of the perpendicular initial energy of the projectile, E_p (eV).

is at least twice higher on the W(100) plane than on the W(110). However, on both planes the qualitative behavior of the ER cross section is similar. The reactivity increases with the perpendicular energy of the projectile up to energies around 2.0 eV (1.8 eV) on the W(100) (W(110)) plane and then decreases up to the highest energy investigated, E_p = 5.0 eV.

Figure 2 highlights the almost negligible impact of the surface temperature on the ER reactivity of hydrogen molecules on both planes. As expected, because of the large mass mismatch between hydrogen and tungsten atoms, the coupling to phonons is very small in agreement with previous work.[30] Therefore, unlike the case of nitrogen[53] on W(100), ER cross sections for hydrogen are almost independent of the surface temperature.

Several opacity maps for the W(100) reticular plane are represented in Figure 3, describing (*X*,*Y*) initial positions (row a in green), and (*X*,*Y*) rebound positions (row b in red), of the projectiles for trajectories leading to ER abstraction. Initial projectile perpendicular energies of 0.1, 1.0, and 3.0 eV are considered for T_s = 300 K. Trajectories leading to ER abstraction involve projectile rebounds in similar areas of the unit cell irrespective of the collision energy. These opacity maps highlight the low ER reactivity for impact parameters *b* close to zero for H+H/W(100), as for most H/H-metal systems with high binding energy of the target.[18,28,72]

Rebounds area are located along lines joining the W atoms and the target adsorption site together with two symmetric rebound areas close to the center of each W(100) square cell. To investigate further the abstraction mechanism, two 2D(*Z*,*Y*)-cuts of the W(100) PES are represented in Figure 4 where the target sits in its equilibrium position and the *X* coordinate of the projectile is set to X_p = 2.5 Å in cut a and X_p = 1.585 Å in cut b. Rebound positions of the projectiles are displayed on the two PES cuts. The calculation performed for E_p = 1.0 eV at T_s = 300 K is selected as an example. On opacity map of Figure 4, the rebound positions of the projectiles close to the center of the cell are now plotted as black dots to be distinguished from the other rebound positions plotted as red dots.

On cut a, the three repulsive structures where the projectile rebounds take place are the top-layer W atom of the cell. This analysis shows that ER mechanism proceeds via collision with the tungsten surface atoms, prior to recombination. ER recombination pathways involving collision with the surface

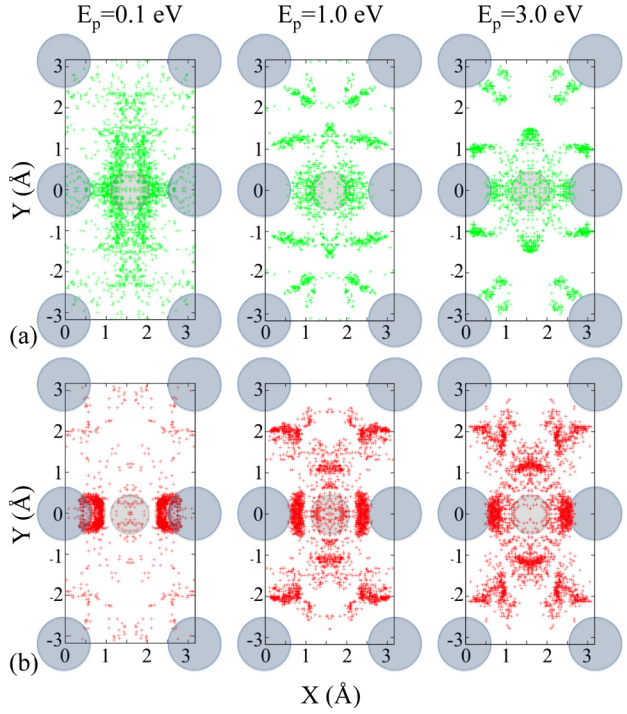

Figure 3. Opacity maps for the W(100) reticular plane: (a) In green, (*X*,*Y*) initial positions of trajectories leading to ER recombination at initial perpendicular energy of the projectile E_p = 0.1, 1.0, and 3.0 eV and a surface temperature T_s = 300 K. (b) In red, (*X*,*Y*) rebound positions of the projectile for the same trajectories leading to ER recombination at the same collision energies. For clarity, only 1/5 of the trajectories have been represented.

atoms were already observed for nitrogen molecules recombination on W(100).[52] On cut b, one repulsive structure is due to the target centered in *Y* = 0.0 Å. The two other repulsive structures, centered in *Y* = 1.585 or −1.585 Å, correspond to the second-layer W atoms. The projectiles with rebound positions in the center of the square cell thus bounce on the subsurface W atoms of the second layer. This mechanism, negligible for E_p = 0.1 eV, contributes up to 16.7% for E_p = 1.0 eV and 24.4% for E_p = 3.0 eV.

Similar opacity maps for W(110) plane are displayed in Figure 5. As for W(110), the ER reactivity for W(100) is small for impact parameters close to zero. Similarly, the reactive areas involved in the ER mechanism are slightly dependent on the initial perpendicular energy of the projectile. Figure 6 displays a two-dimensional cut of the H+H/W(110) PES as a function of the (*Z*,*Y*) position of the projectile over the surface with the target in its equilibrium position and the *X* coordinate of the projectile set to X_p = 1.585 Å. The two symmetric repulsive structures are the top-layer atoms in the center of the W(110) unit cell. The lower repulsive structure centered in *Y* = 0.0 Å is a tungsten atom of the second layer and the circular repulsive structure at *Y* = 0.634 Å and *Z* = 1.096 Å is the target. The rebound positions for ER trajectories, for E_p = 1.0 eV at T_s = 300 K, are represented as black dots. Because of the target equilibrium position, the most attractive part of the potential is located in a range −1.0 Å < Y < 0.0 Å, giving a large window for the projectile to go below the target and catch it in its way back to gas phase after a rebound on the W atom centered in *Y* = −2.24 Å. However, it is interesting that, though energetically possible, the projectiles almost never enter the surface deep enough to bounce on the second layer atom as in

dx.doi.org/10.1021/jp501679n | J. Phys. Chem. C XXXX, XXX, XXX−XXX

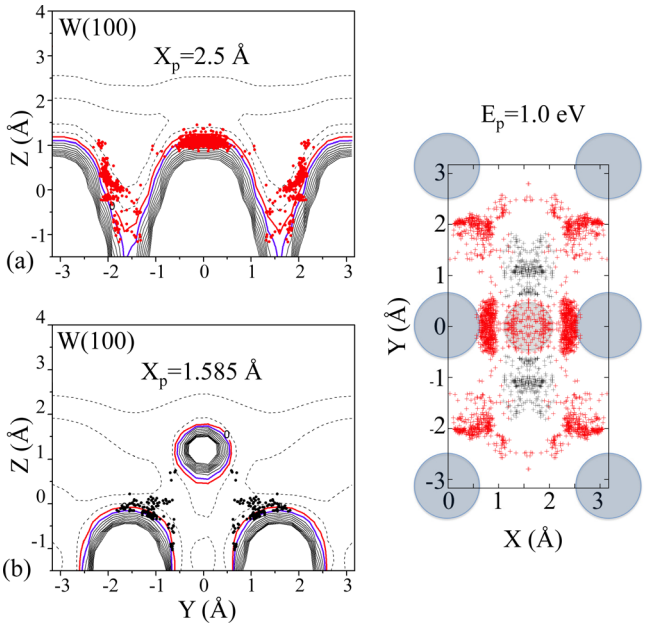

Figure 4. Two-dimensional cuts of the H+H/W(100) PES as a function of the (Z,Y) position of the projectile over the surface. The target sits in its equilibrium position (bridge) and the X coordinate of the projectile is fixed to X_p = 2.5 Å on the cut a and X_p = 1.585 Å on the cut b . Solid and dashed lines are respectively positive and negative isovalues (separated by 1.0 eV). The bold red line is the zero, corresponding to the energy of the target in its equilibrium position and the projectile in gas phase at Z_p = 7.0 Å, and the bold blue line is the 1.0 eV isovalue. The red (black) dots are the rebound positions of the projectiles of trajectories leading to ER recombination for calculation with E_p = 1.0 eV at T_s = 300 K.

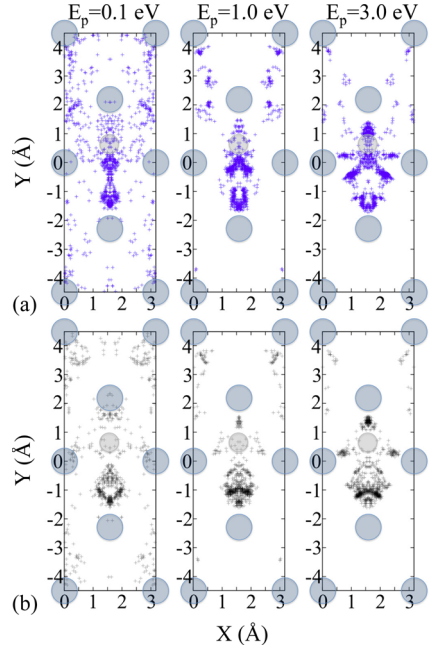

Figure 5. Opacity maps for the W(110) reticular plane: (a) In blue, (X,Y) initial positions of trajectories leading to ER recombination at initial perpendicular energy of the projectile E_p = 0.1, 1.0, and 3.0 eV and a surface temperature T_s = 300 K. (b) In black, (X,Y) rebound positions of the projectile for the same trajectories leading to ER recombination at the same collision energies. For clarity only 1/5 of the trajectories have been represented.

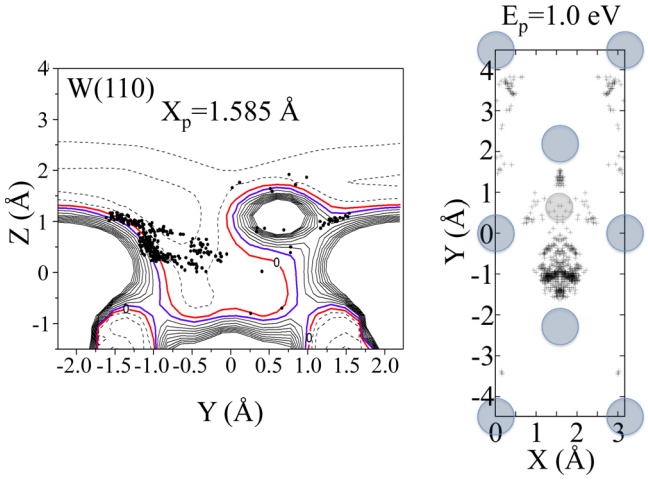

Figure 6. Two-dimensional cut of the H+H/W(110) PES as a function of the (Z,Y) position of the projectile over the surface. The target sits in its equilibrium position, and the X coordinate of the projectile is fixed to X_p = 1.585 Å. Solid and dashed lines are respectively positive and negative isovalues (separated by 1.0 eV). The bold red line is the zero, corresponding to the energy of target in its equilibrium position and the projectile in gas phase at Z_p = 7.0 Å, and the bold blue line is the 1.0 eV isovalue. The black dots are the rebound positions of the projectiles for trajectories leading to ER recombination for E_p = 1.0 eV at T_s = 300 K.

the case on the W(100) plane. This may be related to the second layer position which is located at −1.42 Å on the W(100) plane whereas it is much deeper, −2.16 Å, in the W(110) plane. Moreover, 2D cuts of the potential only give a partial picture of the full dimensional dynamics, and an effect of the target mobility on the hindering of the second layer W atom is possible.

One potential interest in ER abstraction dynamics comes from its ability to form hot products. The adsorption energy of an H atom on a W surface is 3.08 and 3.07 eV, respectively, for W(100) and W(110). The binding energy of H_2 in vacuum is 4.75 eV. Therefore, the ER process is exothermic by 1.67 eV (1.68 eV) on W(100) (W(110)). Thus, the energy available for the formed molecule in the BOSS model is 1.67 eV (1.68 eV) on W(100) (W(110)) plus the ZPE of the target (0.159 eV on W(100) and 0.154 eV on W(110)) plus the initial collision energy of the projectile, E_p. Finally, for E_p = 0.1 eV, on W(100) (W(110)), 1.929 eV (1.934 eV) are available for redistribution into the translational and ro-vibrational degrees of freedom of the recombined H_2 molecule. In Figure 7, the final average translational, rotational, and vibrational energy of the formed H_2 molecules are plotted as a function of the initial perpendicular energy of the projectile, E_p. Most of the available energy is transferred to the translational motion. At low collision energies, internal energy is almost equally shared between rotation and vibration, and then the energy ratio between vibration and rotation increases with E_p. For W(100), the energy transferred into vibration is twice larger than the energy transferred into rotation.

By comparing the W(100) and W(110) surfaces, one important conclusion is the low influence of the reticular plane on the products energy balance. The available energy for partition between the different degrees of freedom is almost identical for both planes. Moreover, the energy partitioning mechanism appears to be insensitive to surface temperature, which confirms the small coupling with the surface phonons

dx.doi.org/10.1021/jp501679n | J. Phys. Chem. C XXXX, XXX, XXX−XXX

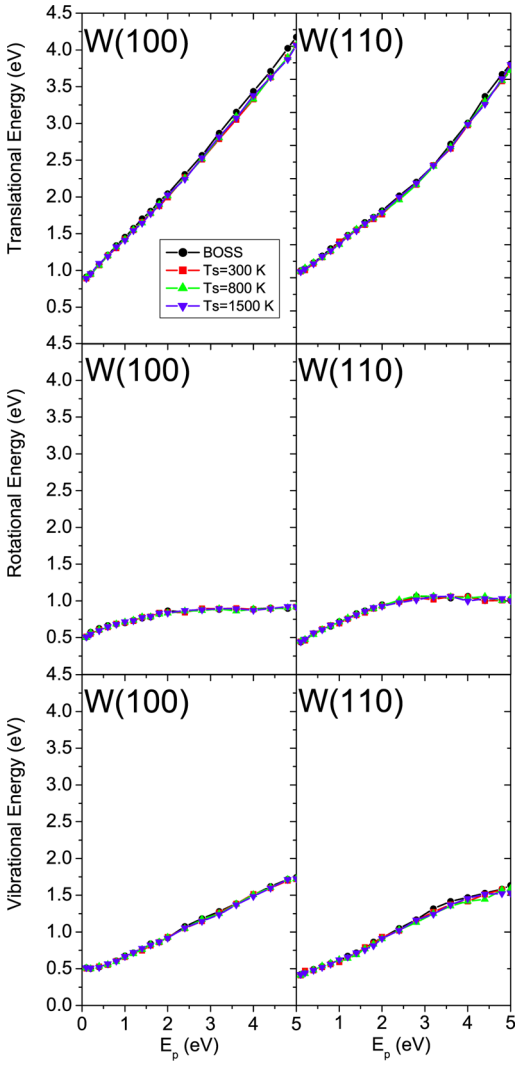

Figure 7. Final average translational (upper panel), rotational (middle panel), and vibrational (lower panel) energies as a function of the perpendicular initial energy of the projectile, E_p (eV).

already observed for the ER cross sections. These results compare well with results of previous theoretical simulations.[30]

4. COMPARISON WITH EXPERIMENTS

As mentioned in Introduction, recently, new H_2 recombination experiments were performed by Markelj et al.[42] In these experiments, a tungsten sample is exposed to hydrogen atoms produced by predissociation of hydrogen molecules on a resistively heated tungsten filament at a temperature of about 2000 K. Then the hydrogen atoms recombine on the sample cooled at 286 K in medium vacuum conditions (10^{-3} mbar). Vibrationally excited hydrogen molecules were found up to $v = 9$, and these highly excited molecules have been attributed to recombination with H atoms adsorbed in low energy binding sites of their polycrystalline tungsten surface. In Figure 8 are represented the relative vibrational populations of the recombined molecules on both PESs and compared to the experimental results. For comparison with experiments, a thermal average of the vibrational populations has been computed following a procedure similar to the one developed in the supplementary file of ref 73 to compute thermally averaged sticking coefficients. Vibrational state distributions

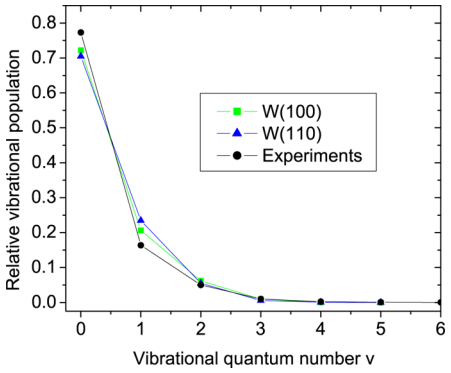

Figure 8. Relative vibrational populations of the recombined molecules. Green squares represent simulation results for the W(100) plane, and blue triangles represent results for the W(110). Experimental results are represented as black dots. Lines are drawn to guide the eye. Experimental results for excitation higher than $v = 6$ (populations about 10^{-4} and lower) are not represented.

have been computed, at normal incidence, for 14 energies in the E_p = 0.05−1 eV range. These distributions have been weighted by the corresponding Eley−Rideal cross sections and thermally averaged assuming a normal energy scaling (NES) or a total energy scaling (TES) regime for ER abstraction cross sections. The vibrational distributions are almost identical within the NES and TES assumptions. We only represent the former ones in the following.

Despite crucial uncertainties concerning the exact nature of the cell surface (polycrystalline surface) or the presence of impurities, our theoretical simulations are in good agreement with the experiments for vibrational populations up to $v = 5$. Populations of levels higher than $v = 3$ are almost negligible. The vibrational excitation determined in this work are also quite similar to the ones of previous theoretical works[13−15] on other systems. The vibrational excitation of the formed molecules appears to be weakly dependent on the temperature and the crystallographic anisotropy. The only significant dependency is found for projectile energy E_p.

5. CONCLUSION

QCT simulations of hydrogen atom normal scattering over a single adsorbate H/W surface are presented for the H+H/W(100) and H+H/W(110) systems. FPLEPS model potentials have been used to reproduce the interactions specificity for both system. In the 0.1−5.0 eV collision energy range, ER abstraction cross sections are found to be small in agreement with previous works on H+H/metal recombination.[18,26,28] The surface temperature effect on ER cross sections and energy partition between the different degrees of freedom of the recombined molecules is almost negligible for both systems. Small ER reactivity is observed at small impact parameters (when the projectile is colliding directly with the target from the gas phase), as already observed for other metals[18,28,72] with high binding energy of the target. Furthermore, ER abstraction pathways proceed via collision of the projectile with the W surface atoms prior to recombination on both systems. However, even if ER cross sections are qualitatively similar for both planes, ER reactivity is twice higher on W(100) than on W(110). For W(100), projectiles bounce on the second layer tungsten atoms before reacting with the target; this mechanism gives a non negligible contribution to the ER reaction cross section (up to 24.4%), underscoring the

dx.doi.org/10.1021/jp501679n | J. Phys. Chem. C XXXX, XXX, XXX−XXX

importance of taking into account the subsurface atoms in the simulations. The formed molecules are found to be ro-vibrationally excited in good agreement with recent experiments. The energy partition between translation, vibration, and rotation is weakly influenced by surface symmetry. Molecule vibrational distributions are in good agreement with experiments conducted at room temperature regardless of the crystallographic plane of W.

AUTHOR INFORMATION

Corresponding Author

*Phone: +33540006310. E-mail: cedric.crespos@u-bordeaux.fr.

Notes

The authors declare no competing financial interest.

REFERENCES

(1) Greenberg, J. M. Cosmic Dust and Our Origins. *Surf. Sci.* **2002**, *500*, 793−822.

(2) Molina, M. J.; Molina, L. T.; Golden, D. M. Environmental Chemistry (Gas and Gas−Solid Interactions): The Role of Physical Chemistry. *J. Phys. Chem.* **1996**, *100*, 12888−12896.

(3) Winnewisser, G.; Herbst, E. Interstellar Molecules. *Rep. Prog. Phys.* **1993**, *56*, 1209−1273.

(4) Mathis, J. S. Observations and Theories of Interstellar Dust. *Rep. Prog. Phys.* **1993**, *56*, 605−652.

(5) Somorjai, G. A. *Introduction to Surface Chemistry and Catalysis*; Wiley: New York, 1994.

(6) Honkala, K.; Hellman, A.; Remediakis, I.; Logadottir, A.; Carlsson, A.; Dahl, S.; Christensen, C.; Norskov, J. Ammonia Synthesis from First-Principles Calculations. *Science* **2005**, *307*, 555−558.

(7) Rayment, T.; Schlögl, R.; Thomas, J. M.; Ertl, G. Structure of the Ammonia Synthesis Catalyst. *Nature* **1985**, *315*, 311−313.

(8) Federici, G.; et al. Key ITER Plasma Edge and Plasma−Material Interaction Issues. *J. Nucl. Mater.* **2003**, *313*, 11−22.

(9) Kleyn, A. W.; Cardozo, N. J. L.; Samm, U. Plasma−Surface Interaction in the Context of ITER. *Phys. Chem. Chem. Phys.* **2006**, *8*, 1761−1774.

(10) Rettner, C. T. Dynamics of the Direct Reaction of Hydrogen Atoms Adsorbed on Cu(111) with Hydrogen Atoms Incident from the Gas Phase. *Phys. Rev. Lett.* **1992**, *69*, 383−386.

(11) Rettner, C. T. Reaction of an H−Atom Beam with Cl/Au(111): Dynamics of Concurrent Eley−Rideal and Langmuir−Hinshelwood Mechanisms. *J. Chem. Phys.* **1994**, *101*, 1529−1546.

(12) Rettner, C. T.; Auerbach, D. J. Dynamics of the Eley-Rideal Reaction of D Atoms with H Atoms Adsorbed on Cu(111): Vibrational and Rotational State Distributions of the HD Product. *Phys. Rev. Lett.* **1995**, *74*, 4551−4554.

(13) Kratzer, P.; Brenig, W. Highly Excited Molecules from Eley-Rideal Reactions. *Surf. Sci.* **1991**, *254*, 275−280.

(14) Jackson, B.; Persson, M. Vibrational Excitation in Recombinative Desorption of Hydrogen on Metal Surfaces: Eley-Rideal Mechanism. *Surf. Sci.* **1991**, *269*, 195−200.

(15) Jackson, B.; Persson, M. A Quantum Mechanical Study of Recombinative Desorption of Atomic Hydrogen on a Metal Surface. *J. Chem. Phys.* **1992**, *96*, 2378−2387.

(16) Shin, H. K. Vibrationally Excited Molecules from the Reaction of H Atoms and Chemisorbed H Atoms on a Metal Surface. *Chem. Phys. Lett.* **1995**, *244*, 235−244.

(17) Persson, M.; Jackson, B. Isotope Effects in the Eley-Rideal Dynamics of the Recombinative Desorption of Hydrogen on a Metal Surface. *Chem. Phys. Lett.* **1995**, *237*, 468−473.

(18) Caratzoulas, S.; Jackson, B.; Persson, M. Eley−Rideal and Hot-Atom Reaction Dynamics of H(g) with H Adsorbed on Cu(111). *J. Chem. Phys.* **1997**, *107*, 6420−6431.

(19) Shalashilin, D. V.; Jackson, B.; Persson, M. Eley−Rideal and Hot-Atom Dynamics of HD Formation by H(D) Incident from the Gas Phase on D(H)-Covered Cu(111). *Faraday Discuss.* **1998**, *110*, 287−300.

(20) Shalashilin, D. V.; Jackson, B.; Persson, M. Eley−Rideal and Hot-Atom Reactions of H(D) Atoms with D(H)-Covered Cu(111) Surfaces: Quasiclassical Studies. *J. Chem. Phys.* **1999**, *110*, 11038−11046.

(21) Kalyanaraman, C.; Lemoine, D.; Jackson, B. Eley−Rideal and Hot-Atom Reactions Between Hydrogen Atoms on Metals: Quantum Mechanical Studies. *Phys. Chem. Chem. Phys.* **1999**, *1*, 1351−1358.

(22) Jackson, B.; Lemoine, D. Eley−Rideal Reactions between H Atoms on Metal and Graphite Surfaces: The Variation of Reactivity with Substrate. *J. Chem. Phys.* **2001**, *114*, 474−482.

(23) Guvenc, Z. B.; Sha, X.; Jackson, B. Eley−Rideal and Hot Atom Reactions between Hydrogen Atoms on Ni(100): Electronic Structure and Quasiclassical Studies. *J. Chem. Phys.* **2001**, *115*, 9018−9027.

(24) Lemoine, D.; Quattrucci, J. D.; Jackson, B. Efficient Eley-Rideal Reactions of H Atoms with Single Cl Adsorbates on Au(111). *Phys. Rev. Lett.* **2002**, *89*, 268302.

(25) Jackson, B.; Sha, X.; Guvenc, Z. B. Kinetic model for Eley−Rideal and Hot Atom Reactions between H Atoms on Metal Surfaces. *J. Chem. Phys.* **2002**, *116*, 2599−2608.

(26) Guvenc, Z. B.; Sha, X.; Jackson, B. The Effects of Lattice Motion on Eley-Rideal and Hot Atom Reactions: Quasiclassical Studies of Hydrogen Recombination on Ni(100). *J. Phys. Chem. B* **2002**, *106*, 8342−8348.

(27) Quattrucci, J. G.; Jackson, B.; Lemoine, D. Eley−Rideal Reactions of H Atoms with Cl Adsorbed on Au(111): Quantum and Quasiclassical Studies. *J. Chem. Phys.* **2003**, *118*, 2357−2365.

(28) Martinazzo, R.; Assoni, S.; Marinoni, G.; Tantardini, G. F. Hot-Atom versus Eley−Rideal Dynamics in Hydrogen Recombination on Ni(100). I. The Single-Adsorbate Case. *J. Chem. Phys.* **2004**, *120*, 8761−8771.

(29) Lanzani, G.; Martinazzo, R.; Materzanini, G.; Pino, I.; Tantardini, G. F. Chemistry at Surfaces: from Ab Initio Structures to Quantum Dynamics. *Theor. Chem. Acc.* **2007**, *117*, 805−825.

(30) Rutigliano, M.; Cacciatore, M. Eley-Rideal Recombination of Hydrogen Atoms on a Tungsten Surface. *Phys. Chem. Chem. Phys.* **2011**, *13*, 7475−7484.

(31) Bechu, S.; Bes, A.; Lemoine, D.; Pelletier, J.; Bacal, M. Investigation of H^- production by surface interaction of the plasma generated in "Camembert III" reactor via distributed electron cyclotron resonance at 2.45 GHz. *Rev. Sci. Instrum.* **2008**, *79*, 02A505.

(32) Bechu, S.; Lemoine, D.; Bacal, M.; Bes, A.; Pelletier, J. Production of H^- Ions by Surface Mechanisms in Cs-free Multi-dipolar Microwave Plasma. *AIP Conf. Proc.* **2009**, *74*, 1097−2008.

(33) Kammler, T.; Wehner, S.; Küppers, J. The Role of Sticking and Reaction Probabilities in Hot-Atom Mediated Abstraction Reactions of D on Metal Surfaces by Gaseous H Atoms. *J. Chem. Phys.* **1998**, *109*, 4071−4077.

(34) Kammler, T.; Kolovos-Vellianitis, D.; Küppers, J. A Hot-Atom Reaction Kinetic Model for H Abstraction from Solid Surfaces. *Surf. Sci.* **2000**, *460*, 91−100.

(35) Kim, J. Y.; Lee, J. Kinetics, Mechanism, and Dynamics of the Gas-Phase H(D) Atom Reaction with Adsorbed D(H) Atom on Pt(111). *J. Chem. Phys.* **2000**, *113*, 2856−2865.

(36) Harris, J.; Kasemo, B. On Precursor Mechanisms for Surface Reactions. *Surf. Sci.* **1981**, *105*, L281−L287.

(37) Eley, D. D.; Rideal, E. K. Parahydrogen Conversion on Tungsten. *Nature* **1940**, *146*, 401−402.

(38) Eley, D. D. The Interchange of Hydrogen in the Adsorbed Film on Tungsten. *Proc. R. Soc. London A* **1941**, *178*, 452−464.

(39) Eley, D. D.; Rideal, E. K. The Catalysis of the Parahydrogen Conversion by Tungsten. *Proc. R. Soc. London A* **1941**, *178*, 429−451.

(40) Hall, R. I.; Cadez, I.; Landau, M.; Pichou, F.; Shermann, C. Vibrational Excitation of Hydrogen via Recombinative Desorption of Atomic Hydrogen Gas on a Metal Surface. *Phys. Rev. Lett.* **1988**, *60*, 337−340.

(41) Eenshuistra, P. J.; Bonnie, J. H. M.; ans Hopman, J. L. H. J. Observationof Exceptionally High Vibrational Excitation of Hydrogen

Molecules Formed by Wall Recombination. *Phys. Rev. Lett.* **1988**, *60*, 341−344.
(42) Markelj, S.; Cadez, I. Production of Vibrationally Excited Hydrogen Molecules by Atom Recombination on Cu W Materials. *J. Chem. Phys.* **2011**, *134*, 124707.
(43) Barnes, M. R.; Willis, R. F. Hydrogen-Adsoprtion-Induced Reconstruction of Tungsten (100): Observation of Surface Vibrational Modes. *Phys. Rev. Lett.* **1978**, *41*, 1729−1733.
(44) White, J. A.; Bird, D. M.; Payne, M. C. Dissociation of H_2 on W(100). *Phys. Rev. B* **1996**, *53*, 1667−1674.
(45) Busnengo, H. F.; Martinez, A. E. H_2 Chemisorption on W(100) and W(110) Surfaces. *J. Phys. Chem. C* **2008**, *112*, 5579−5588.
(46) Kammler, T.; Lee, J.; Küppers, J. A Kinetic Study of the Interaction of Gaseous H(D) Atoms with D(H) Adsorbed on Ni(100) Surfaces. *J. Chem. Phys.* **1997**, *106*, 7362−7371.
(47) Wehner, S.; Küppers, J. Abstraction of D Adsorbed on Pt(111) Surfaces with Gaseous H Atoms. *J. Chem. Phys.* **1998**, *108*, 3353−3359.
(48) Kammler, T.; Küppers, J. Interaction of H Atoms with Cu(111) Surfaces: Adsorption, Absorption and Abstraction. *J. Chem. Phys.* **1999**, *111*, 8115−8123.
(49) Kolovos-Vellianitis, D.; Kammler, T.; Küppers, J. Interaction of Gaseous H atoms with Cu(100) Surfaces: Adsorption, Absorption, and Abstraction. *Surf. Sci.* **2000**, *454*−*456*, 316.
(50) Wehner, S.; Küppers, J. Abstraction of H Adsorbed on Pt(111) Surfaces with Gaseous D Atoms: Isotope and Flux Effects. *Surf. Sci.* **1998**, *411*, 46−53.
(51) Zecho, T.; Brandner, B.; Küppers, J. Abstraction of D Adsorbed on Pt(100) Surfaces by Gaseous H Atoms: Effect of Surface Heterogeneity. *Surf. Sci. Lett.* **1998**, *418*, L26−L30.
(52) Quintas-Sánchez, E.; Larrégaray, P.; Crespos, C.; Martin-Gondre, L.; Rubayo-Soneira, J.; Rayez, J.-C. Dynamical Reaction Pathways in Eley-Rideal Recombination of Nitrogen from W(100). *J. Chem. Phys.* **2012**, *137*, 064709.
(53) Quintas-Sánchez, E.; Crespos, C.; Rayez, J.-C.; Martin-Gondre, L.; Rubayo-Soneira, J. Surface Temperature Effects on the Dynamics of N_2 Eley-Rideal Recombination on W(100). *J. Chem. Phys.* **2013**, *138*, 024706.
(54) Nienhaus, H. Electronic Exitations by Chemical Reactions on Metal Surfaces. *Surf. Sci. Rep.* **2002**, *45*, 1−78.
(55) Martin-Gondre, L.; Crespos, C.; Larrégaray, P.; Rayez, J.-C.; van Ootegem, B.; Conte, D. Is the LEPS Potential Accurate Enough to Investigate the Dissociation of Diatomic Molecules on Surfaces? *Chem. Phys. Lett.* **2009**, *471*, 136−142.
(56) Martin-Gondre, L.; Crespos, C.; Larrégaray, P.; Rayez, J.-C.; Conte, D.; van Ootegem, B. Detailed Description of the Flexible Periodic London−Eyring−Polanyi− Sato Potential Energy Function. *Chem. Phys.* **2010**, *367*, 136−147.
(57) Martin-Gondre, L.; Crespos, C.; Larrégaray, P.; Rayez, J.-C.; van Ootegem, B.; Conte, D. Dynamics Simulation of N_2 Scattering onto W(100,110) Durfaces: A Stringent Test for the Recently Developed Flexible Periodic London−Eyring−Polanyi−Sato Potential Energy Surface. *J. Chem. Phys.* **2010**, *132*, 204501.
(58) Busnengo, H. F.; Salin, A.; Dong, W. Representation of the 6D Potential Energy Surface for a Diatomic Molecule near a Solid Surface. *J. Chem. Phys.* **2000**, *112*, 7641−7651.
(59) Olsen, R. A.; Busnengo, H. F.; Salin, A.; Somers, M. F.; Kroes, G. J.; Baerends, E. J. Constructing Accurate Potential Energy Surfaces for a Diatomic Molecule Interacting with a Solid Surface: H_2 + Pt (111) and H_2 + Cu (100). *J. Chem. Phys.* **2002**, *116*, 3841−3857.
(60) Kresse, G. Dissociation and sticking of H_2 on the Ni(111), (100), and (110) substrate. *Phys. Rev. B* **2000**, *62*, 8295−8305.
(61) Adelman, S. A. Generalized Langevin Theory for Manybody Problems in Chemical Dynamics: General Formulation and the Equivalent Harmonic Chain Representation. *J. Chem. Phys.* **1979**, *71*, 4471−4486.
(62) Tully, J. C. Dynamics of Gas-Surface Interactions: 3D Generalized Langevin Model Applied to fcc and bcc Surfaces. *J. Chem. Phys.* **1980**, *73*, 1975−1985.
(63) Dohle, M.; Saalfrank, P.; Uzer, T. The Dissociation of Diatomic Molecules on Vibrating Surfaces: A Semiclassical Generalized Langevin Approach. *J. Chem. Phys.* **1998**, *108*, 4226−4236.
(64) Polanyi, J. C.; Wolf, R. J. Dynamics of Simple Gas-Surface Interaction. II. Rotationally Inelastic Collisions at Rigid and Moving Surfaces. *J. Chem. Phys.* **1985**, *82*, 1555−1566.
(65) Busnengo, H. F.; Dong, W.; Salin, A. Trapping, Molecular Adsorption, and Precursors for Nonactivated Chemisorption. *Phys. Rev. Lett.* **2004**, *93*, 236103.
(66) Ernst, H.-J.; Hulpke, E.; Toennies, J. P. Helium-Atom-Scattering Study of the Structure and Phonon Dynamics of the W(001) Surface between 200 and 1900 K. *Phys. Rev. B* **1992**, *46*, 16081−17007.
(67) Titmuss, S.; Wander, A.; King, D. A. Reconstruction of Clean and Adsorbate-Covered Metal Surfaces. *Chem. Rev.* **1996**, *96*, 1291−1306.
(68) Alnot, P.; Cassuto, A.; King, D. A. Adsorption and Desorption Kineticks with No Precursor Trapping: Hydrogen and Deuterium on W(100). *Surf. Sci.* **1989**, *215*, 29−46.
(69) Ho, W.; Willis, R. F.; Plummer, E. W. Obersvation of Nondipole Electron Impact Vibrational Excitations: H on W(100). *Phys. Rev. Lett.* **1978**, *40*, 1463−1466.
(70) Balden, M.; Lehwald, S.; Ibach, H.; Mills, D. L. Hydrogen Coverred W(110) Surface: A Hydrogen Liquid with a Propensity for One-Dimensional Order. *Phys. Rev. Lett.* **1994**, *73*, 854−857.
(71) Balden, M.; Lehwald, S.; Ibach, H. Substrate and Hydrogen Phonons of the Ordered p (2 × 1) and (2 × 2) Phase and the Anomalous (1 × 1) Phase of Hydrogen on W(110). *Phys. Rev. B* **1996**, *53*, 7479−7491.
(72) Jackson, B.; Persson, M. Effects of Isotopic Substitution on Eley−Rideal Reactions and Adsorbate-Mediated Trapping. *J. Chem. Phys.* **1995**, *103*, 6257−6279.
(73) Ramos, M.; Minniti, M.; Díaz, C.; Miranda, R.; Martin, F.; Martinez, A. E.; Busnengo, H. F. Environment-driven reactivity of H_2 on Pd Ru surface alloys. *Phys. Chem. Chem. Phys.* **2013**, *15*, 14936−14940.